

Christiaan J.J. Paredis and Pradeep K. Khosla,  
“Fault Tolerant Task Execution Through Global Trajectory Planning”  
to appear in *Reliability Engineering and System Safety*, December 1996.

# Fault Tolerant Task Execution through Global Trajectory Planning

Christiaan J. J. Paredis      Pradeep K. Khosla

Department of Electrical and Computer Engineering and  
The Robotics Institute,  
Carnegie Mellon University,  
Pittsburgh, Pennsylvania 15213.

## Abstract

*Whether a task can be completed after a failure of one of the degrees-of-freedom of a redundant manipulator depends on the joint angle at which the failure takes place. It is possible to achieve fault tolerance by globally planning a trajectory that avoids unfavorable joint positions before a failure occurs. In this article, we present a trajectory planning algorithm that guarantees fault tolerance while simultaneously satisfying joint limit and obstacle avoidance requirements.*

## 1 Introduction

Reliability is becoming an essential attribute of robot manipulators in a growing range of applications, such as space missions, nuclear waste retrieval, and medical robotics. This trend has spawned a research effort in fault tolerant robotics, covering topics ranging from fault detection and identification [16] to design [11, 13], control [5, 15], and redundancy resolution [6] of fault tolerant manipulators.

Fault tolerance is the ability of a system to continue normal operation despite the presence of failures in subsystems. This can be achieved by adding redundancy at different levels of the system. Sreevijayan [13] proposed a four-level subsumptive architecture for actuation redundancy in fault tolerant robot manipulators:

Level 1: Dual actuators—extra actuators per joint,

Level 2: Parallel structures—extra joints per DOF,

Level 3: Redundant manipulators—extra DOFs per manipulator arm,

Level 4: Multiple arms—extra arms per manipulator system.

A system designed with redundancies at all four levels can possibly sustain multiple simultaneous faults.

An example of a fault tolerant design for the space shuttle manipulator is described in [17]. Fault tolerance is here guaranteed by using a differential gear train with dual input actuators for every DOF—an implementation of the first level of the four-level subsumptive architecture. In this article, we propose a method to achieve fault tolerance using redundant DOFs (Level 3). We define a manipulator to be 1-fault tolerant if it can complete its task even if one of its joints fails and is immobilized [11]. This definition is based on the following scenario:

A fault detection and identification algorithm monitors the proper functioning of each degree-of-freedom (DOF) of a redundant manipulator. As soon as it detects a failure of a subcomponent, an intelligent controller immobilizes the corresponding DOF by activating its brake, and automatically adapting the joint trajectory to the new manipulator structure. The task is then continued without interruption.

According to this scenario, a large variety of possible faults, ranging from sensor faults to transmission and actuation faults, can be treated in exactly the same manner, namely, by eliminating the whole DOF through immobilization.

Whether a task can be completed after a joint failure depends not only on the structure of the manipulator [12], but also on the specific joint angle at which the failure occurs. In general, failures at a fully extended or folded back position of a joint are most detrimental to the remaining capabilities of the manipulator. The basic idea that we exploit in this article is to achieve fault tolerance by avoiding unfavorable joint positions *before* failure. This idea was first proposed in [6] where the null-space component of a redundant manipulator was used to locally minimize the kinematic fault tolerance measure (kfm)<sup>1</sup>. The authors showed that, for a particular test path, a manipulator with kfm minimization is more likely to be fault tolerant than a

---

1. The kinematic fault tolerance measure, or kfm, is defined as the minimum dexterity after joint failure.

manipulator with traditional pseudoinverse control. However, due to the local nature of the kfm, fault tolerance could not be guaranteed globally [7].

In this article, we present a trajectory planning algorithm that guarantees fault tolerance on a global scale, while avoiding any violations of secondary kinematic requirements such as joint limits and obstacles. To achieve this global result, we have to consider the topology of the self-motion manifolds, as has been previously suggested in [7, 8].

The redundancy provisions needed for fault tolerance can be incorporated only at the price of increased complexity. This drawback can be overcome by a modular and structured design philosophy, as is advocated in [5, 10, 14]. Modularity in hardware and software has the advantage of facilitating testing during the design phase and therefore reducing the chances for unanticipated faults. Modules also constitute natural boundaries to which faults can be confined. By including fault detection and recovery mechanisms in critical modules, the effect of local faults remains internal to the modules, totally transparent to the higher levels of the manipulator system. Such a modular design philosophy is embodied in the Reconfigurable Modular Manipulator System (RMMS) developed in the Advanced Manipulators Laboratory at Carnegie Mellon University [10]. The RMMS utilizes a stock of interchangeable link modules of different lengths and shapes, and joint modules of various sizes and performance specifications. By combining these general purpose modules, a wide range of manipulator configurations can be assembled. In Section 6, a simulation of the RMMS is used to illustrate our global trajectory planning algorithm.

## 2 Definitions

In this section, we introduce several concepts that are essential for the development of the algorithm presented in the next section. We start by giving an exact definition of the problem.

### ***Definition 1: Fault Tolerant Trajectory Planning Problem***

Given: - a manipulator defined by its geometry, joint limits, and redundancy resolution algorithm.

– a task description consisting of a Cartesian path,  $p(t) \in \mathfrak{R}^m$ , and the geometry of the obstacles.

Find: – a fault tolerant trajectory in joint space<sup>2</sup>:  $\theta(t) \in T^n$ .

A fault tolerant trajectory is defined as follows:

***Definition 2: Fault Tolerant Trajectory***

A trajectory,  $\theta(t) \in T^n$ , is 1-fault tolerant with respect to the task of following the Cartesian path  $p(t) \in \mathfrak{R}^m$ , if for every DOF,  $j = 1 \dots n$ , and for every instant,  $t^*$ , there exists an alternate trajectory,  $\theta(t, j, t^*)$ , for which:

- 1)  $\theta(t, j, t^*)$  maps onto  $p(t)$  under the forward kinematics
- 2)  $\theta(t^*) = \theta(t^*, j, t^*)$
- 3)  $\theta_j(t, j, t^*) = \theta_j(t^*), \quad \forall t > t^*$
- 4)  $\theta(t, j, t^*)$  does not violate any secondary task requirements such as joint limits or obstacles.

This definition corresponds to our scenario for fault tolerance as described in the introduction. Before any failures occur, the manipulator follows the fault tolerant joint trajectory  $\theta(t)$ . After a failure in joint  $j$  at time  $t^*$ , joint  $j$  is immobilized and the joint trajectory is adapted to keep tracking the path  $p(t)$ . The new trajectory,  $\theta(t, j, t^*)$ , is equal to  $\theta(t)$  at the instant of failure and maintains a constant joint angle,  $\theta_j(t^*)$ , for the frozen joint  $j$  after the failure.

There are an infinite number of alternate trajectories,  $\theta(t, j, t^*)$ , one for every possible combination of a failing DOF and an instant of failure. This poses practical problems. While one can explicitly store a discretized version of  $\theta(t)$ , explicit storage of all  $\theta(t, j, t^*)$  is impossible. Therefore, we assume that the alternate trajectories are stored *implicitly* in a redundancy resolution algorithm that computes  $\theta(t, j, t^*)$  at run time once a failure has taken place. We also assume that this redundancy resolution algorithm unambiguously determines  $\theta(t, j, t^*)$ , given  $t^*$ ,  $\theta(t^*)$ , and  $j$ ; that is, we only consider redundancy resolution algorithms that

---

2. We assume that the manipulator has only revolute joints. The joint space is therefore the  $n$ -dimensional torus  $T^n$ .

determine the next joint vector based on the current joint vector, and not on past joint vectors. This assumption is satisfied for commonly used Jacobian-based algorithms of the form:

$$\dot{\theta} = J^{\dagger}\dot{x} + (I - J^{\dagger}J)\dot{\Phi}. \quad (1)$$

Readers unfamiliar with this kind of redundancy resolution algorithms are referred to [9] for a detailed overview; an example is also given in Section 6 of this article.

Because the choice of the redundancy resolution algorithm fully determines the alternate trajectories, it also influences the solution of the trajectory planning problem. In this article, we assume the redundancy resolution algorithm to be a given of the problem, i.e., a part of the manipulator definition. Consequently, for a failure of joint  $j$  at posture  $\theta(t^*)$ , there exists a unique alternate trajectory  $\theta(t, j, t^*)$ .

In the fourth point of the definition of a fault tolerant trajectory, we refer to “secondary task requirements.” The primary requirement is to follow the path  $p(t)$ . In the problem definition, we included joint limits and obstacles as secondary requirements, but one can include any other kinematic requirement that only depends on the current posture. For instance, all the dexterity measures enumerated in [4] depend only on the current joint position and could thus be included as secondary requirements. We call the set of postures that satisfy all the secondary task requirements the set  $S$ .

At each instant,  $t$ , the manipulator postures  $\theta(t)$  and  $\theta(t, j, t^*)$  map onto the path  $p(t)$  under the forward kinematics of the manipulator,  $p = f(\theta)$ . Consequently, we say that these postures are elements of the preimage of  $p$ .

***Definition 3: Preimage of a point  $p$***

The preimage of a point,  $p$ , is the set  $\Sigma(p) = \{\theta \in T^n \mid f(\theta) = p\}$ , where  $f$  is the forward kinematic mapping of the manipulator.

This preimage is a set of  $r$ -dimensional manifolds,<sup>3</sup> where  $r = n - m$  is the degree-of-redundancy of the manipulator.

---

3. An exception is the preimage of a critical value, which is not a manifold but a bouquet of tori [1].

Assume now that joint  $j$  fails. We call the resulting manipulator, with joint  $j$  immobilized, a reduced order derivative (ROD).

**Definition 4:  $k$ -Reduced Order Derivative**

A manipulator with  $(n - k)$  DOFs, obtained by immobilizing  $k$  of the joints of an  $n$ -DOF manipulator, is called a  $k$ -reduced order derivative.

Whether this ROD is able to complete the task, as is required for fault tolerance, depends on the posture  $\theta(t^*) \in \Sigma(p(t^*))$  at which the failure occurred. For certain  $\theta(t^*)$ , the path  $p(t)$  might pass outside the workspace of the ROD, the redundancy resolution algorithm might get stuck at a singularity, or the alternate trajectory  $\theta(t, j, t^*)$  might violate the joint limits or cause a collision with an obstacle. In all of these cases, the task cannot be completed. We call the corresponding posture  $\theta(t^*)$  intolerant to a failure of DOF  $j$ .

**Definition 5: Posture Tolerant to a Failure of DOF  $j$**

A posture  $\theta \in \Sigma(p(t^*))$  is tolerant to a failure of DOF  $j$  if and only if the alternate trajectory  $\theta(t, j, t^*)$ , as determined by the redundancy resolution algorithm, satisfies all the task requirements.

We call the set of postures  $\theta \in \Sigma(p(t^*))$  that are tolerant to a failure of DOF  $j$  the set  $F_j^{t^*} \subset \Sigma(p(t^*))$ .

Based on the definition of a fault tolerant trajectory, we conclude that a posture is an acceptable posture for a fault tolerant trajectory if it is tolerant to failures of each of the DOFs. The set of acceptable postures  $\theta \in \Sigma(p(t^*))$  is given by the equation:

$$A^{t^*} = \bigcap_{j=1}^n F_j^{t^*}. \tag{2}$$

### 3 Algorithm

The algorithm to determine a fault tolerant trajectory consists of two parts. In the first part, we determine for each instant,  $t^*$ , the set of acceptable postures,  $A^{t^*}$ , as defined in the previous

section. In the second part, we create a connectivity graph for the acceptable postures and search this graph to determine a fault tolerant trajectory.

A key observation for the development of our algorithm is that whether a posture,  $\theta(t^*)$ , is acceptable depends only on the future course of the path  $p(t)$ ; it is independent of  $p(t)$  for  $t < t^*$ . For example, if a failure occurs at the last point,  $p_{last}$ , of the path, the task can always be completed, regardless of which course the path followed previously and regardless of the posture in which the manipulator reaches this last point. We conclude that

$$\lambda^{t_{last}} = F_1^{t_{last}} = \dots = F_n^{t_{last}} = \Sigma(p_{last}) \cap \xi. \quad (3)$$

This conclusion forms the basis for the algorithm's initialization.

The main iteration of our algorithm is based on a second important observation. Consider a candidate fault tolerant trajectory,  $\theta_1(t)$ . At time  $t_1$ , joint  $j$  fails and the alternate trajectory  $\theta_1(t, j, t_1)$  is followed, as is illustrated in Figure 1. Consider also a second candidate fault tolerant trajectory,  $\theta_2(t)$ , which intersects with  $\theta_1(t, j, t_1)$  at time  $t_2$ , so that  $\theta_1(t_2, j, t_1) = \theta_2(t_2)$ . If a failure of joint  $j$  were to occur at time  $t_2$ , the alternate trajectory  $\theta_2(t, j, t_2)$  would be followed. Because the joint velocity,  $\dot{\theta}$ , in the redundancy resolution algorithm, depends only on  $j$ ,  $p(t)$ , and the current joint vector, the two alternate trajectories

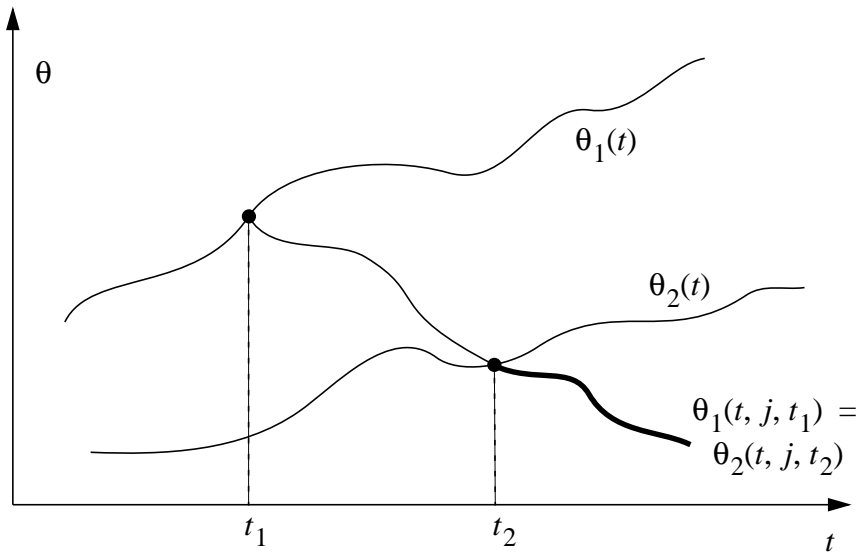


**Figure 1:** Two possible failures resulting in the same alternate trajectory.

$\theta_1(t, j, t_1)$  and  $\theta_2(t, j, t_2)$  are equal to each other for  $t > t_2$ . A Corollary of this observation is that a posture is tolerant to a fault in joint  $j$  if and only if all the postures along the corresponding alternate trajectory are also tolerant to faults in joint  $j$ :

$$\begin{aligned} \exists(t_1) \in F_j^{t_1} &\Leftrightarrow \theta(t^*, j, t_1) \in F_j^{t^*}, \\ \forall t^* > t_1 \text{ and } \theta(t_1) \in S \end{aligned} \quad (4)$$

which is equivalent to the expression:

$$\begin{aligned} \theta(t_1) \in F_j^{t_1} &\Leftrightarrow \theta(t^*, j, t_1) \in F_j^{t^*}, \\ \forall t^* \in (t_1, t_1 + \Delta t] \text{ and } \theta(t_1) \in S, \Delta t > 0 \end{aligned} \quad (5)$$

Equation (5) means that we can determine whether a posture,  $\theta(t_1)$ , is tolerant to a fault of DOF  $j$  by tracing the alternate trajectory up to  $t_1 + \Delta t$  rather than up to  $t_{last}$ . This property is used in the main iteration of the first part of our algorithm.

**Part 1:** determination of the acceptable postures

- discretize the path:  $p_k = p(t_k) = p(k\Delta t)$
- compute the preimage of the last point:  $\Sigma(p_{last})$
- compute the acceptable postures for the last point:  $A^{t_{last}} = F_j^{t_{last}} = \Sigma(p_{last}) \cap S$
- for  $k=last-1$  to  $first$  do
  - compute the preimage:  $\Sigma(p_k)$
  - for  $j=1$  to  $n$  do
    - for every posture  $\theta \in \Sigma(p_k)$  do
      - compute  $\theta(t_{k+1}, j, t_k)$  using the  
redundancy resolution algorithm
      - if  $\theta \in S$  and  $\theta(t_{k+1}, j, t_k) \in F_j^{t_{k+1}}$  then  $\theta \in F_j^{t_k}$
    - next  $\theta$
  - next  $j$
  - compute the set of acceptable postures:  $A^{t_k} = \bigcap_{j=1}^n F_j^{t_k}$
- next  $k$



Once the sets of acceptable postures have been computed, a fault tolerant trajectory is chosen in the second part of our algorithm. A fault tolerant trajectory consists of a sequence,  $\{\theta(t_k)\}$  of acceptable postures—one posture  $\theta(t_k) \in A^{t_k}$  for each instant  $t_k$ . However, one cannot pick the postures  $\theta(t_k)$  at random from  $A^{t_k}$ . For a valid fault tolerant sequence, there should exist a continuous trajectory of acceptable postures connecting each pair of postures  $\theta(t_k)$  and  $\theta(t_{k+1})$ . Moreover, the sequence  $\{\theta(t_k)\}$  should preferably vary smoothly and stay away from the boundaries of  $A^{t_k}$ . To simplify the search for such a sequence, we first group the postures of  $A^{t_k}$  that are connected to each other.

In general, a set,  $A^{t_k}$ , may consist of several disjoint regions,  $R_i^{t_k}$ , of acceptable postures:

$$A^{t_k} = \bigcup R_i^{t_k} \quad \text{and} \quad R_i^{t_k} \cap R_j^{t_k} = \emptyset, \quad \forall i \neq j. \quad (6)$$

The postures in each region  $R_i^{t_k}$  are connected to each other in the sense that there exists a continuous trajectory of acceptable postures,  $\theta \in A^{t_k}$ , connecting any two postures in  $R_i^{t_k}$ . On the other hand, by definition, there does not exist any combination of two postures, one from  $R_i^{t_k}$  and one from  $R_j^{t_k}$ , for which such a continuous trajectory can be found. Similarly, we call two regions  $R_i^{t_k}$  and  $R_j^{t_{k+1}}$  connected if there exists a continuous trajectory of acceptable postures,  $\theta(t)$ , with  $t \in [t_k, t_{k+1}]$ , connecting any two postures  $\theta_i \in R_i^{t_k}$  and  $\theta_j \in R_j^{t_{k+1}}$ . As a result, a fault tolerant trajectory exists if and only if there exists a sequence of connected regions,  $\left\{ R_i^{t_1}, \dots, R_j^{t_{last}} \right\}$ . This result is used in the second part of our algorithm, in which we build a connectivity graph representing the connections between the regions  $R_i^{t_k}$ . The structure of this graph is in general very simple due to the limited number of disjoint regions in each  $A^{t_k}$ , and due to the limited number of connections between regions at time  $t_k$  and regions at time  $t_{k+1}$ . It is possible that there exists no fault tolerant sequence of connected regions. To achieve fault tolerance in this case, the manipulator itself needs to be adapted by changing its structure, joint limits, or redundancy resolution algorithm.

In the final step of the algorithm, a fault tolerant trajectory is determined from the sequence of connected regions. In general, there are an infinite number of possible fault tolerant trajectories. However, a good trajectory should vary smoothly and stay away from the boundaries of the

regions  $\mathbb{R}_j^{t,k}$ . The choice of one specific fault tolerant trajectory can be further limited by imposing additional task requirements or objectives.

**Part 2:** search for a fault tolerant trajectory

- for  $k=last$  to  $first$  do
  - group the acceptable postures,  $\mathbb{A}^{t,k}$ , in disjoint regions  $\mathbb{R}_i^{t,k}$
  - for each region  $\mathbb{R}_i^{t,k}$ , determine the connections with the regions for  $k+1$
  - store in connectivity graph
- next  $k$
- search the connectivity graph to determine a fault tolerant sequence of the regions  $\mathbb{R}_i^{t,k}$
- select a fault tolerant trajectory

## 4 Implementational issues

Although most of the steps of the algorithm, presented in the previous section, can be easily implemented, the computation of the preimage,  $\Sigma(p)$ , requires some further explanation. As mentioned before, for an  $n$ -DOF manipulator, the preimage of a point,  $p \in \mathbb{R}^m$ , is a set of  $r$ -dimensional manifolds in the  $n$ -dimensional torus  $T^n$ , where  $r = n - m$  is the degree-of-redundancy of the manipulator. The preimage is defined implicitly by the forward kinematics function  $f(\theta) = p$ . The computation of the preimage involves translating this implicit representation into an explicit one, for example, a random sampling of the preimage stored as a finite set of postures  $\theta \in T^n$ . However, this particular representation is insufficient for our algorithm because it does not capture the topology of the preimage. Topological information is needed in three steps of the algorithm: first, where the sets  $\mathbb{F}_j^{t,k}$  are computed; second, where the intersection of these sets is taken to obtain  $\mathbb{A}^{t,k}$ ; and third, where the acceptable postures are grouped into disjoint regions  $\mathbb{R}_j^{t,k}$ . It is important to notice that in all three instances only the local topology matters. Locally, an  $r$ -dimensional manifold is diffeomorphic to  $\mathbb{R}^r$ , and can thus be approximated by an  $r$ -dimensional hyperplane. Therefore, we have chosen to represent the preimage  $\Sigma(p)$  by a polygonal approximation consisting of line segments when  $r = 1$ , or

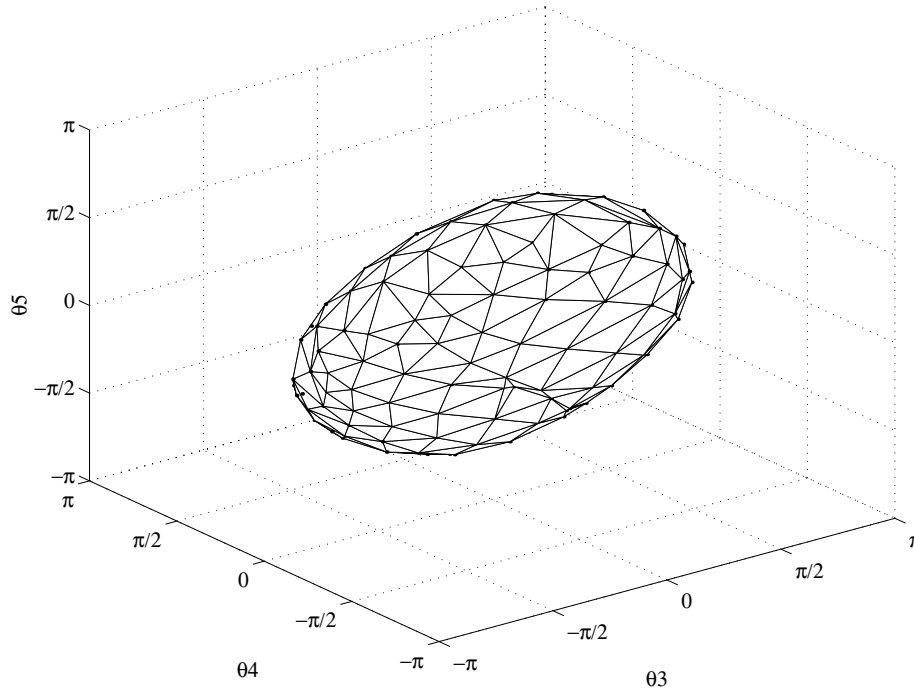


**Figure 2:** The projection onto the  $(\theta_3, \theta_4, \theta_5)$ -space of a polygonal approximation of a 2-dimensional preimage for a 5-DOF manipulator.

triangular patches when  $r = 2$ , as is illustrated in Figure 2. Let  $S$  be the number of postures  $\theta \in T^n$  used to approximate  $\Sigma(p)$ , then  $S$  increases as the accuracy of the approximation increases.  $S$  also depends on the dimensionality,  $r$ , of the preimage; this dependency is *exponential*.

The algorithm also requires the Cartesian path  $p(t)$  to be approximated by a sequence  $\{p_k\}$  with  $p_k = p(k\Delta t)$ . Let  $P$  be the number of points in the sequence  $\{p_k\}$ . Just like  $S$ ,  $P$  depends on the accuracy of the approximation. In this case, the dependency is always linear because the Cartesian path is 1-dimensional.

The complexity of the algorithm is mainly determined by the nested loop of the first part of the algorithm. Assuming that the complexity of the redundancy resolution algorithm is linear in  $n$ , the complexity of our trajectory planning algorithm can be expressed as:

$$P \cdot n \cdot S \cdot O(n) \quad \text{or} \quad P \cdot e^r \cdot O(n^2). \quad (7)$$

Because of the exponential dependency on  $r$ , the algorithm is only practical for  $r = 1$  or  $r = 2$ . Fortunately, two degrees-of-redundancy are sufficient to achieve fault tolerance in most practical applications [11].

## 5 Illustrative example

In this section, we illustrate the use of the fault tolerant trajectory planning algorithm with an example of a 3-DOF planar manipulator. This simple example enables us to describe graphically how a fault tolerant trajectory is selected.

The 3-DOF manipulator has 3 links of length 1; the joint limits are  $\pm 100^\circ$  for  $\theta_1$  and  $\pm 150^\circ$  for  $\theta_2$  and  $\theta_3$ ; no redundancy resolution algorithm is specified because the 2-DOF reduced order derivatives are non-redundant. The task is to follow the trajectory shown in Figure 3 at constant speed in a total time of 10 seconds; a circular obstacle is centered at  $(0.7, 0)$  and has a radius of 0.2.

Because the manipulator in this example has one degree-of-redundancy,  $r = 1$ , the preimage of every point,  $p(t)$ , is a one dimensional subset of  $T^3$  and can be parametrized as  $\Sigma(p(t)) = g(p(t), \alpha)$  with  $\alpha \in T^1$ . The function  $g$  describes a 2-dimensional surface in  $T^3$ , as illustrated in Figure 4. The surface can be parametrized by two parameters: the Cartesian

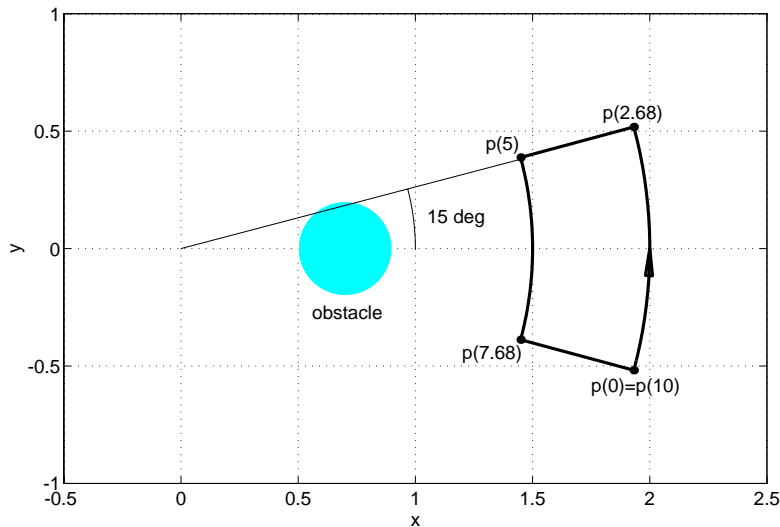


**Figure 3:** The Cartesian path and obstacle position.

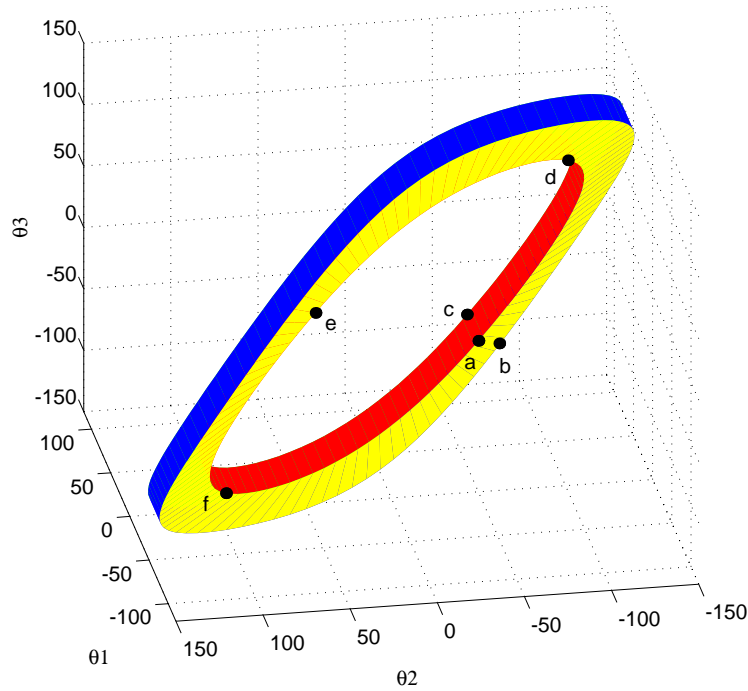


**Figure 4:** The preimage of the trajectory.

posture	$\theta_1$ [deg]	$\theta_2$ [deg]	$\theta_3$ [deg]	$t$ [sec]	$\alpha$ [rad]
a	45.00	-60.00	-60.00	0 and 10	0 or $2\pi$
b	75.00	-60.00	-60.00	2.68	0 or $2\pi$
c	61.52	-75.52	-75.52	7.68	0 or $2\pi$
d	13.95	-104.48	104.48	0 and 10	$\pi/2$
e	-75.00	60.00	60.00	0 and 10	$\pi$
f	-43.95	104.48	-104.48	0 and 10	$3\pi/2$

**Table 1:** The coordinates for each of the postures labeled a–f in Figure 4:  
 Joint angles  $\theta_1$ ,  $\theta_2$ , and  $\theta_3$ : the coordinates for the 3D representation of the preimage (Figure 4)  
 time  $t$  and preimage parameter  $\alpha$ : the coordinates for the 2D representation of the preimage (Figures 5–8)

position  $p$  (or time  $t$ ), and the preimage parameter  $\alpha$ . The postures labeled  $a$ ,  $d$ ,  $e$ , and  $f$ , are all part of the preimage of the same point,  $p(0)$  (or  $p(10)$ ). The postures labeled  $a$ ,  $b$ , and  $c$ , on the other hand, have the same value for the preimage parameter,  $\alpha = 0$  (or  $\alpha = 2\pi$ ), but map onto different points,  $p$ , along the path. One can also unwrap this surface and represent it in a planar coordinate system with the time in abscissa and the preimage parameter  $\alpha$  in ordinate<sup>4</sup>; this representation is used in Figures 5 through 8. Table 1 gives the coordinates of the six postures,  $a$  through  $f$ , for both the three-dimensional and the two-dimensional representations of Figures 4 and 5, respectively.

In the first part of the algorithm, the sets  $F_j^{t_k}$  are determined. They are depicted in Figures 5 through 7 as the white areas. The dark gray areas are postures that do not satisfy the secondary task requirements; i.e., they are the sets  $\Sigma(p(t)) - S$ . These postures would be unacceptable for a joint trajectory even if fault tolerance were not required. The light gray area is the set of postures for which the alternate trajectories do not meet the task requirements. The alternate trajectories  $\theta(t, j, t_k)$  for this example are totally determined by keeping the joint angle  $\theta_j$  constant, and are represented by the black curves. Notice that, for the postures in the light gray area, the alternate trajectories either pass through a posture that violates a secondary task requirement, or get stuck at a singularity and do not reach the end of the path. In either case, the requirement for fault tolerance is violated. The sets of acceptable postures  $A^{t_k}$  are indicated in white in Figure 8. This white area is the intersection of the white areas in Figures 5, 6 and 7, in accordance with Equation (2).

In the second part of our algorithm, the acceptable postures are first grouped into disjoint regions. Such a region,  $R_i^{t_k}$ , corresponds to a vertical white line segment with abscissa  $t_k$  in Figure 8. The number of disjoint regions is usually small—a maximum of six for this example. Once the regions  $R_i^{t_k}$  have been determined, the connections with the disjoint regions at time  $t_{k+1}$  are stored in a connectivity graph, which is shown in Figure 9. As mentioned before, the graph is very simple in general. For this example, there exists only one fault tolerant sequence of connected regions. A possible fault tolerant trajectory for this sequence is shown as a dashed

---

4. Keep in mind that the planar representation does not capture the exact topology of the 2-dimensional surface, because the preimage parameter  $\alpha$  is an element of  $T^1$  and the path  $p(t)$  is closed,  $p(0) = p(10)$ .

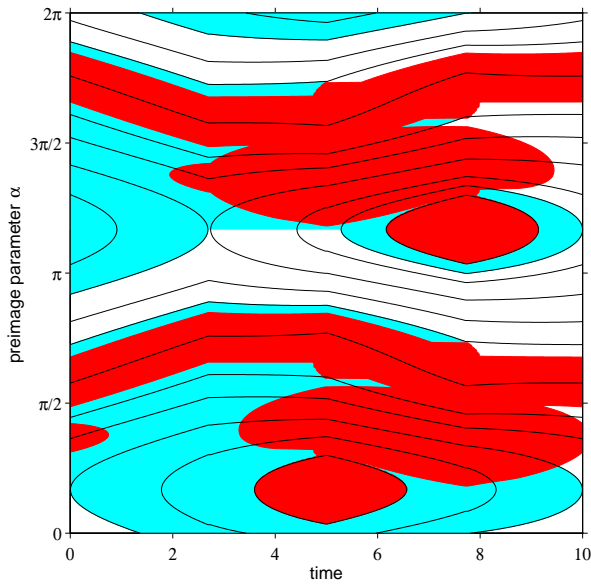


**Figure 5:** The set of postures tolerant to a fault in joint 1 (in white).

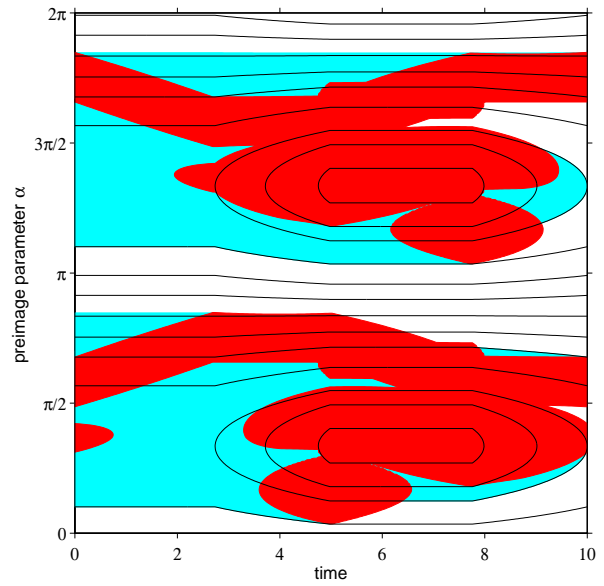


**Figure 6:** The set of postures tolerant to a fault in joint 2 (in white).

The dark gray areas are postures that violate the secondary task requirements (joint limits and obstacles). The light gray areas are postures for which the alternate trajectory violates the task requirements. The black curves are alternate trajectories, determined by keeping the angle of the failing joint constant.

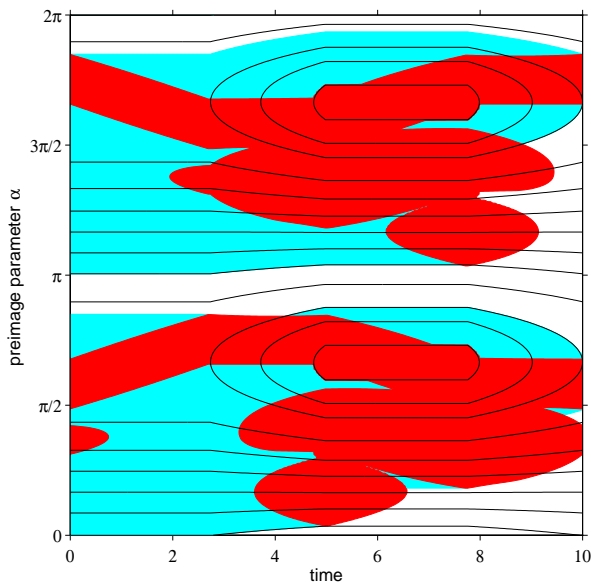


**Figure 7:** The set of postures tolerant to a fault in joint 3 (in white).

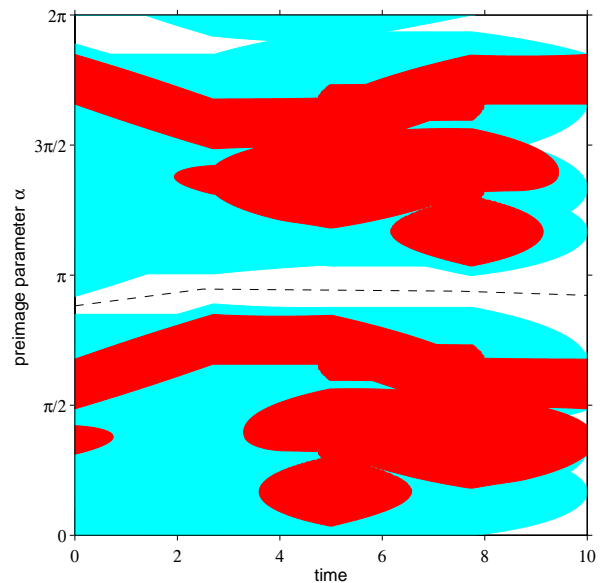


**Figure 8:** A possible fault tolerant trajectory (dashed line). The white areas are the sets of acceptable postures.

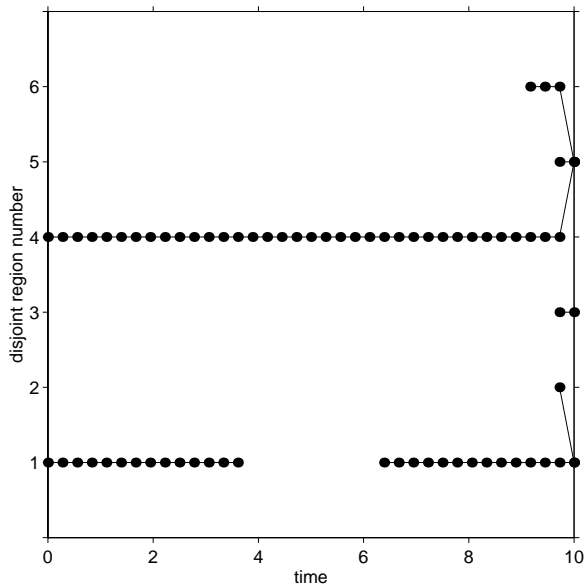


**Figure 9:** Connectivity graph for the disjoint regions of acceptable postures.

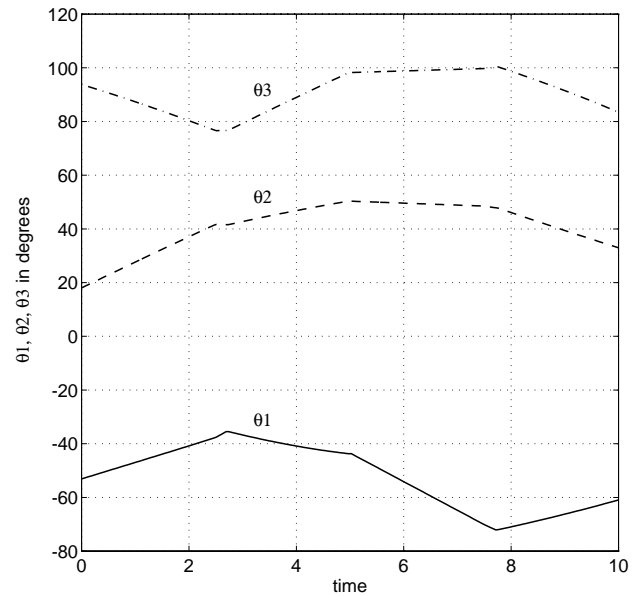


**Figure 10:** Fault tolerant trajectories for the individual joints.

line in Figure 8. The corresponding individual joint trajectories are depicted in Figure 10.

## 6 Comprehensive example

In this section, we describe an example of fault tolerant task execution by the 4-DOF spatial manipulator shown in Figure 11. The manipulator is a configuration of the Reconfigurable Modular Manipulator System (RMMS), and consists of the manipulator base, three pivot joint modules, one rotate joint module, and a link module. The modules are assembled such that the resulting manipulator has the Denavit-Hartenberg parameters listed in Table 2. The joint limits for each of the joint modules are  $\pm 165^\circ$ . The task is to follow a circular path on a table while avoiding collisions with the table—even after one of the joint modules has failed and is immobilized.

The simulation uses the same control software running on the same hardware as would be used to control the actual manipulator system. The only difference is that the robot interface is replaced by an interface to the TeleGrip simulation software package (by Deneb Inc.). TeleGrip runs on a SGI Crimson which is connected to the VME-based control hardware through a VME-



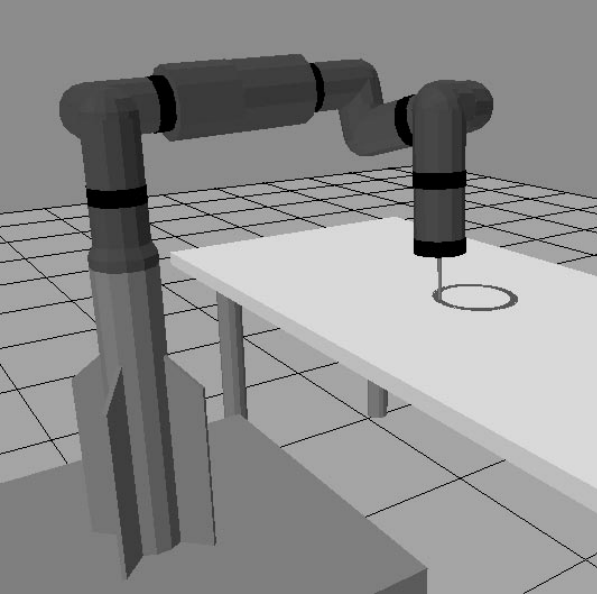


**Figure 11:** A simulation of the Reconfigurable Modular Manipulator System executing a fault tolerant trajectory.

dof	link offset	link length	twist angle
1	-0.1373	0.0	$\pi/2$
2	0.7344	0.0	$\pi/2$
3	-0.1373	0.3270	$-\pi/2$
4	-0.1373	0.4705	0.0

**Table 2:** Denavit-Hartenberg parameters.  
 (in meters and radians)

to-VME-adaptor. We use a damped least-squares kinematic controller with null-space optimization:

$$\dot{\theta} = J^*(\dot{p} + \alpha(p - x)) + \beta(I - J^*J)(\theta_{ft} - \theta) , \quad (8)$$

where  $J^*$  is the singularity robust Jacobian inverse [3],  $p(t)$  is the desired Cartesian path, and  $\theta_{ft}(t)$  is the fault tolerant trajectory. The null-space optimization component of the controller ensures that the manipulator follows the desired fault tolerant joint space trajectory closely before a failure occurs, as is shown in Figure 12. After failure, the same controller is used with the column of the Jacobian, which corresponds to the frozen joint, set to zero. The trajectories for the remaining joints deviate from the fault tolerant trajectory to ensure that the end effector continues to track the desired path.

Instead of using the kinematic controller given by Equation (8), one could linearly interpolate the fault tolerant trajectory before failure and only switch to Cartesian control after failure. Besides having to switch controllers at the instant of failure, this has the disadvantages that a dense

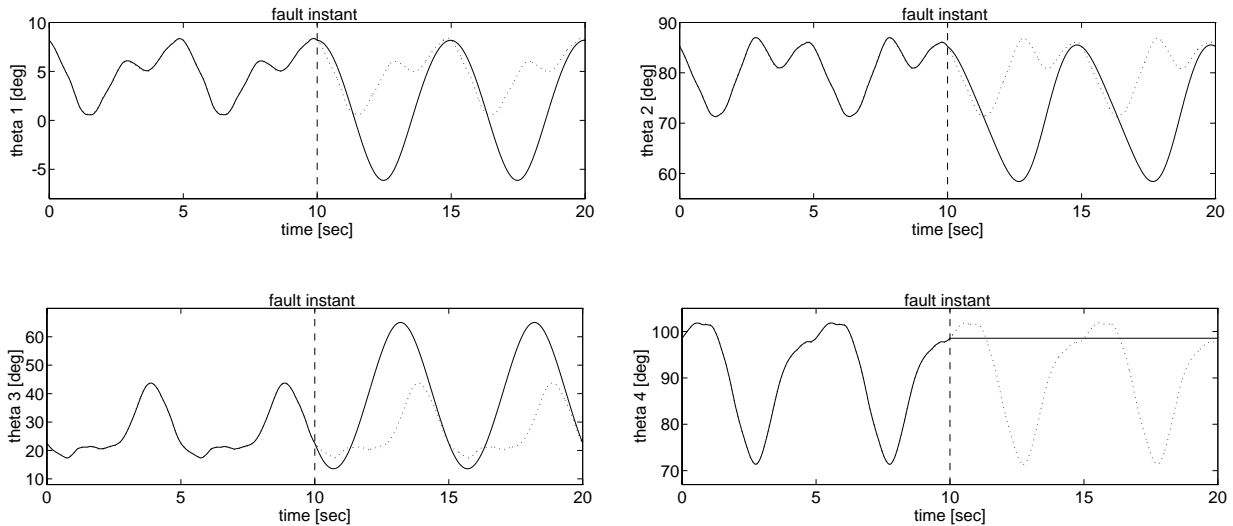


**Figure 12:** Joint trajectories theta 1 through theta 4. Before failure (0–10sec), the manipulator follows the fault tolerant trajectory. At the tenth second, joint 4 fails and is immobilized. The manipulator then deviates from the fault tolerant trajectory (dotted line) and follows the alternate trajectory (solid line) as determined by the redundancy resolution algorithm.

sampling of the fault tolerant trajectory is required to achieve good end effector position accuracy. Furthermore, Equation (8) allows us to move back smoothly to the fault tolerant trajectory if the failure was temporary.

Figure 13 shows the position error of the end effector. The error does not increase after failure and remains an order of magnitude smaller than the distance traveled by the end effector during

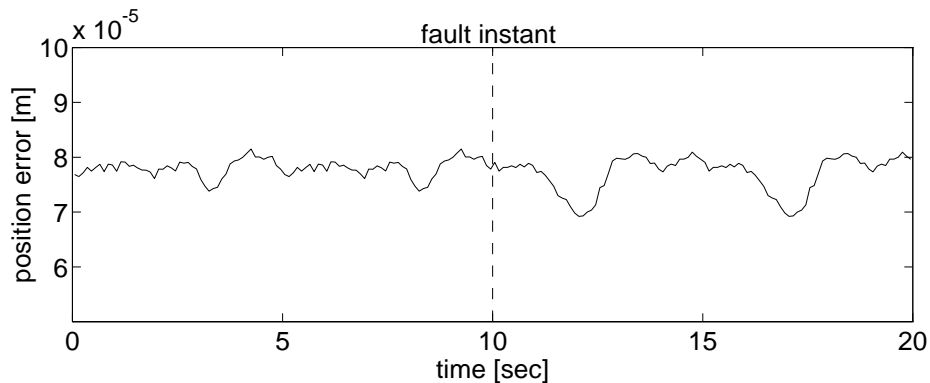


**Figure 13:** The end effector position error does not increase after failure.

one sample period:

$$s = \frac{2\pi \cdot 0.1 \text{ m}}{5 \text{ sec} \cdot 150 \text{ Hz}} = 8.38 \times 10^{-4} \text{ m} \gg \text{error} \quad (9)$$

The error could be further reduced by increasing the cycle frequency of the damped least-squares controller.

Many simulations with a wide variety of failure times and failing joints resulted in a maximum positional error of  $8.67 \times 10^{-5} \text{ m}$ . This confirms the fact that the trajectory determined by our algorithm is indeed fault tolerant with respect to this task. Unfortunately, we cannot demonstrate this graphically as we did for the previous example. Because the topology of the preimage changes at the points where the path crosses the critical value manifolds of the manipulator [1], the preimage of the path cannot be unfolded into a 2-dimensional graph such as Figure 8.

## 7 Comparison

In this section, we compare our algorithm for global fault tolerant trajectory planning with the approaches for fault tolerant task execution described in [6], [7], and [11].

In [6], the authors propose a local redundancy resolution algorithm which maximizes the kinematic fault tolerance measure,  $kfm^5$ . The  $kfm$  is defined as the minimum remaining dexterity of the manipulator after joint failure:

$$kfm = \min_{f=1..n} \sigma_m({}^f J), \quad (10)$$

where  $\sigma_m({}^f J)$  is the smallest singular value of the Jacobian of the original manipulator with the  $f$ -th column removed. One can think of the dexterity,  $\sigma_m$ , as the ease with which the end-effector of the manipulator can be moved in the least suitable direction. To achieve fault tolerance, it is important that, after a joint fails and is immobilized, all end-effector movements remain feasible, that is,  $\sigma_m$  remains non-zero. This idea is realized practically by using a redundancy resolution algorithm with null-space maximization of the  $kfm$ . Due to the local

---

5. The authors also define a dynamic fault tolerance measure,  $dfm$ , which we do not consider in this article.

nature of the kinematic fault tolerance measure, however, this method cannot guarantee fault tolerance on a global scale. Moreover, it does not take secondary requirements such as joint limits and obstacles into consideration. Nevertheless, the method is important in case the desired end-effector path is unknown a priori; global off-line path planning is impossible in this case, so that local optimization of the  $kfm$  combined with joint limit and obstacle avoidance, is probably the best one can do. A drawback of the method is that it requires the computation of the gradient of the  $kfm$ , which in turn requires the computation of the full singular value decomposition of  ${}^f J$ ; the computational complexity for the singular value decomposition of an  $m \times n$  matrix is approximately [2]

$$4m^2n + 8mn^2 + 9n^3. \quad (11)$$

Although this is quite computationally intensive for an on-line algorithm, it does not suffer from exponential complexity in the degree-of-redundancy,  $r$ , so that this method could be used to achieve local fault tolerance even in highly redundant manipulators.

In [7], Lewis and Maciejewski acknowledge the local nature of the  $kfm$  approach and propose a global method for fault tolerant task execution. For every “critical task point” (a point that needs to be reachable after joint failure), a bounding box of the preimage manifold is computed. Every critical task point is reachable after joint failure, if the failure occurs at a posture inside the intersection of the bounding boxes of the preimage manifolds. Global fault tolerance is achieved by using a redundancy resolution algorithm that ensures that the joint space trajectory remains inside the intersection of the bounding boxes. This method is similar to our global fault tolerant trajectory planning algorithm to the extent that it uses the pre-computation of the preimage manifolds to achieve global fault tolerance. However, since it only uses the *bounding boxes* of the preimage manifolds, it cannot guarantee path following. This drawback is illustrated with the comprehensive example of Section 6. The desired Cartesian path passes through the two points,  $p_1 = (0.763, 0.393, 0.783)$  and  $p_2 = (0.895, 0.331, 0.783)$ . Assume that the point  $p_1$  is reached in the posture  $\vec{\theta}_1$ , which is inside the bounding boxes of the preimages of  $p_1$  and  $p_2$ , as is shown in Figure 14. A failure occurs in joint 1, locking it at  $\theta_1 = -45^\circ$ . To reach the point  $p_2$ , the manipulator would have to move to either  $\vec{\theta}_2$  or  $\vec{\theta}_3$ , both of which would

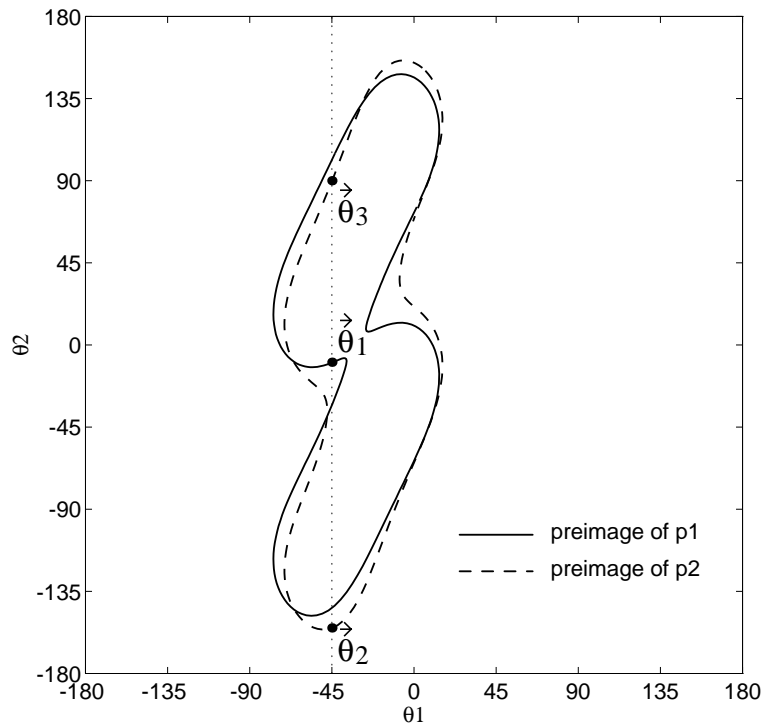


**Figure 14:** A case in which the method described in [7] cannot guarantee fault tolerant path following.

require a deviation from the desired path. On the contrary, in our global trajectory planning algorithm,  $\vec{\theta}_1$  is not an acceptable posture because a failure of joint one would result in the redundancy resolution algorithm getting stuck at a singularity. Another disadvantage of the method described in [7] is that, just like in [6], secondary requirements are not taken into account. Also, the algorithm requires the computation of the preimage manifolds which is, as we have shown before, exponential in the degree-of-redundancy,  $r$ ; this limits the usefulness of the algorithm to manipulators with  $r = 1$  or  $2$ .

A third approach to fault tolerant task execution is described in [11]. This approach is different because it does not make any assumptions about the redundancy resolution algorithm used at run-time. Instead, fault tolerance is achieved at the design stage. A manipulator is designed which is able to reach every task point even when an arbitrary joint fails at an arbitrary angle. As a result of the assumption that a joint can fail at an *arbitrary* angle, at least two degrees-of-redundancy, instead of one, are necessary for 1-fault tolerance. An additional drawback is that the design algorithm does not consider obstacles—it does take joint limits into account.

Moreover, it only guarantees reachability of task points, not path following.

In conclusion, the two main qualities that distinguish our fault tolerant trajectory planning algorithm from the other approaches to fault tolerant task execution are its ability to guarantee fault tolerance for path following, and its consideration of secondary requirements.

## **8 Summary**

We have presented a trajectory planning algorithm for fault tolerant task execution. This algorithm guarantees fault tolerance on a global scale, while also satisfying secondary kinematic task requirements such as joint limits and obstacles. The algorithm consists of two main parts. In the first part, the postures acceptable for a fault tolerant trajectory are determined. The computations are based on the topology of the preimages of the Cartesian path, and on the characteristics of the redundancy resolution algorithm which is used after a failure has occurred. In the second part of the algorithm, a connectivity graph is constructed, representing the topological structure of the set of acceptable postures. By searching this graph, a global fault tolerant trajectory is found. A simple example for a 3-DOF planar manipulator is used to explain the development of the algorithm graphically. A second more comprehensive example further illustrates some of the kinematic control issues of fault tolerant task execution. Compared to other approaches for fault tolerant task execution, our method has the advantage that it guarantees fault tolerance for path following, and that it takes secondary requirements such as joint limits and obstacles into consideration.

## **Acknowledgment**

This research was funded in part by the Department of Energy under grant DOE-F902-89ER14042, by Sandia under contract AL-3020, by the Department of Electrical and Computer Engineering, and by The Robotics Institute, Carnegie Mellon University.

## References

- [1] J. W. Burdick, “Kinematic Analysis and Design of Redundant Robot Manipulators,” Stanford Computer Science Report no. STAN-CS-88-1207, 1988.
- [2] G. H. Golub and C. F. Van Loan, *Matrix Computations (second edition)*, Baltimore: The Johns Hopkins University Press, 1989.
- [3] L. Kelmar and P. K. Khosla, “Automatic Generation of Forward and Inverse Kinematics for a Reconfigurable Modular Manipulator System,” *Journal of Robotic Systems*, Vol. 7, No. 4, pp. 599–619, 1990.
- [4] J.-O. Kim and P. K. Khosla, “Dexterity Measures for Design and Control of Manipulators,” in *Proceedings of the IEEE/RSJ International Workshop on Intelligent Robots and Systems (IROS'91)*, pp. 758–763, Osaka, Japan, November 1991.
- [5] S. Kotosaka et al., “Fault Tolerance of a Functionally Adaptive and Robust Manipulator,” in *Proceedings of the 1993 IEEE/RSJ International Conference on Intelligent Robots and Systems (IROS'93)*, pp. 294–300, Yokohama, Japan, July 26–30, 1993.
- [6] C. L. Lewis and A. A. Maciejewski, “Dexterity Optimization of Kinematically Redundant Manipulators in the Presence of Joint Failures,” *Computers and Electrical Engineering*, Vol. 20, No. 3, pp. 273–288, 1994.
- [7] C. L. Lewis and A. A. Maciejewski, “An Example of Failure Tolerant Operation of a Kinematically Redundant Manipulator,” in *Proceedings of the 1994 IEEE International Conference on Robotics and Automation*, pp 1380–1387, San Diego, California, May 1994.
- [8] C. L. Lück and S. Lee, “Global Path Planning of Redundant Manipulators Based on Self-

- Motion Topology,” in *Proceedings of the 1994 IEEE International Conference on Robotics and Automation*, pp. 372–377, San Diego, California, May 1994.
- [9] D. N. Nenchev, “Redundancy Resolution through Local Optimization: A Review,” *Journal of Robotic Systems*, Vol. 6, No. 6, pp. 769–798, 1989.
- [10] C. J. J. Paredis et al., “A Rapidly Deployable Fault Tolerant Manipulator System,” in *Proceedings of the Workshop on Some Critical Issues in Robotics*, Singapore, 2–3 October, 1995.
- [11] C. J. J. Paredis and P. K. Khosla, “Mapping Tasks into Fault Tolerant Manipulators,” in *Proceedings of the 1994 IEEE International Conference on Robotics and Automation*, pp. 696–703, San Diego, California, May 1994.
- [12] C. J. J. Paredis and P. K. Khosla, “Design of Modular Fault Tolerant Manipulators,” to appear in *The Algorithmic Foundations of Robotics*, eds. K. Goldberg et al., Boston, Massachusetts: A.K. Peters, 1995.
- [13] D. Sreevijayan, *On the Design of Fault-Tolerant Robotic Manipulator Systems*, M.S. Thesis, Mechanical Engineering Department, The University of Texas at Austin, June 1992.
- [14] D. Tesar and M. S. Butler, “A Generalized Modular Architecture for Robot Structures,” *Manufacturing Review*, Vol 2, No. 2, pp. 91–118, 1989.
- [15] Y. Ting, S. Tosunoglu, and D. Tesar, “Control Algorithms for Fault-Tolerant Robots,” in *Proceedings of the 1994 IEEE International Conference on Robotics and Automation*, pp. 910–915, San Diego, California, May 1994.
- [16] M. L. Visinsky, I. D. Walker, and J. R. Cavallaro, “New Dynamic Model-Based Fault



Christiaan J.J. Paredis and Pradeep K. Khosla,  
“Fault Tolerant Task Execution Through Global Trajectory Planning”  
to appear in *Reliability Engineering and System Safety*, December 1996.

Detection Thresholds for Robot Manipulators,” in *Proceedings of the 1994 IEEE International Conference on Robotics and Automation*, San Diego, California, pp. 1388-1395, May 1994.

- [17]E. C. Wu, J. C. Hwang, and J. T. Chladek, “Fault-Tolerant Joint Development for the Space Shuttle Remote Manipulator System: Analysis and Experiment,” *IEEE Transactions on Robotics and Automation*, Vol. 9, No. 5, pp. 675–684, 1995.